Contract No:

This document was prepared in conjunction with work accomplished under Contract No. DE-AC09-08SR22470 with the U.S. Department of Energy (DOE) Office of Environmental Management (EM).

Disclaimer:

We put science to work.™

Savannah River National Laboratory®

OPERATED BY SAVANNAH RIVER NUCLEAR SOLUTIONS

A U.S. DEPARTMENT OF ENERGY NATIONAL LABORATORY • SAVANNAH RIVER SITE • AIKEN, SC

2020 Report - SRNL Aging and Lifetimes program tritium aging studies on structural alloys

Including joint studies with SNL/CA

Timothy M. Krentz

January 2021

SRNL-STI-2021-00046, Revision 0

SRNL.DOE.GOV

DISCLAIMER

Printed in the United States of America

Prepared for
U.S. Department of Energy

Keywords: *Mechanical Properties, Type 304L Stainless Steel, Type 21-6-9 Stainless Steel, Hydrogen, Tritium, Helium, Embrittlement*

Retention: *Permanent*

2020 Report - SRNL Aging and Lifetimes program tritium aging studies on structural alloys

Timothy M. Krentz

January 2021

Prepared for the U.S. Department of Energy under contract number DE-AC09-08SR22470.

Savannah River National Laboratory®

OPERATED BY SAVANNAH RIVER NUCLEAR SOLUTIONS

ACKNOWLEDGEMENTS

Joe Ronevich of Sandia National Laboratories prepared and provided the weld and HAZ specimens as well as the tensile and tube specimens for tritium pre-charging. He also provided results on hydrogen exposed samples of the weld and HAZ specimens, as well as valuable technical discussion and feedback. Vanessa Cofer and Kellie Holland performed vital Material Control and Accountability assistance. Chad Sweeney, Lane Rogers, Calvin Clamp, Anne Kelly, Dante Pilgrim, and Mauricio Martinez made invaluable contributions in preparing tritium charging vessels and tritium charging procedures; conducting specimen recovery; and transporting specimens to SRNL after tritium precharging runs. Dale Hitchcock and Dustin Olson conducted the TPD measurements, and Dale Hitchcock also provided valuable technical review.

EXECUTIVE SUMMARY

This report documents work performed in calendar year 2020 at SRNL in support of the Aging and Lifetimes program. This work is part of an on-going collaboration between SRNL and SNL to understand tritium embrittlement of structural metals in Gas Transfer System reservoirs which informs lifetime assessments and lifetime predictions. In this effort, test coupons are precharged with tritium and allowed to age in a freezer to minimize tritium egress and allow for born-in helium levels to systematically increase. Coupons are then removed periodically and tested to develop an understanding of how mechanical properties degrade as helium levels increase. This report summarizes test results from coupons which are in various stages of aging as they were tritium precharged in previous years.

In 2020, a series of tests were performed on 304L that was previously tritium precharged and allowed to age to nominally 100 appm helium. Tensile testing of heat treated 304L tubes (and welded tubes) aged to 100 appm helium were completed which provided a unique study of a diverse set of microstructures and yield strengths ranging from 200-800 MPa. This work was developed into a conference paper co-authored with SNL. Additionally, 304L notched and smooth tensile specimens aged to 100 appm helium were tensile tested to predetermined amounts of strain to provide for a systematic microscopy investigation of aging effects on microstructural damage in partnership with SNL. Austenitic stainless steel weld and heat affected zone fracture specimens were tested in the aged condition (nominally 600 appm helium) and the results are compared to previous results which were aged to nominally 300 appm helium. The fracture measurements show a decrease in fracture resistance with increasing helium buildup. A tritium precharging run was performed in 2020 on 304L electron (E-beam) weld coupons as well as 21-6-9 annealed coupons. The coupons will be aged and tested at select helium contents over the comings months and years to develop and understanding of material degradation with increasing aging time. Table 0-1 provides the status of the ongoing tritium coupon aging studies. The table includes the year tritium precharing took place, the material, and the targeted helium concentrations (appm) for testing.

Also documented are initial commissioning tests on a new thermally programmed desorption (TPD) instrument, being set up for measuring the trapping and de-trapping processes of hydrogen in these materials. This technique may yield valuable new insight to how hydrogen interacts with the metal’s atomic lattice on a thermodynamic basis.

Table 0-1. Status of Ongoing Tritium Coupon Aging Programs

		Mechanical Testing of Aged Specimens with Born-in Helium (appm)				
Material	**Tritium Precharged (year)**	**100**	**200**	**300**	**600**	**1000**
304L weld/HAZ	2017	DNM	NP	Complete	Complete	Planned
21-6-9 weld/HAZ*	2017	DNM	NP	Complete	Complete	Planned
304L tube, tensile	2019	Complete	NP	Planned	Planned	Planned
304L E-beam welds	2020	Planned	NP	Planned	Planned	Planned
21-6-9 Annealed	2020	Planned	Planned	Planned	Planned	Planned

DNM = did not measure
NP = not planned
**21-6-9 HAZ will have higher Helium concentrations due to higher solubility for tritium*

TABLE OF CONTENTS

LIST OF TABLES

LIST OF FIGURES

LIST OF ABBREVIATIONS

SRNL	Savannah River National Laboratory
SNL (/CA)	Sandia National Laboratories (California campus)
FZ	Fusion Zone (as of a weld)
HAZ	Heat Affected Zone (as of a weld)
appm	Atomic parts per million
TDS	Thermal Desorption Spectroscopy
TPD	Thermally Programmed Desorption

1.0 Introduction

Tritium reservoirs are constructed from forged stainless steels and filled at the Savannah River Site. Austenitic stainless steels are chosen for their good compatibility with hydrogen isotopes, as they are resistant, but not immune, to embrittlement from hydrogen isotopes. This embrittlement occurs when hydrogen and its isotopes dissolve into the metal's atomic lattice and alter deformation processes, embrittling the materials. Additionally, the helium from tritium decay becomes trapped in the microstructure, creating nanoscale bubbles and further reducing resistance over the service life of the material. Cracks have been observed in storage vessels after extended service [1-5]. The consequences of a leak in service are high, and thus information on changing mechanical properties over time is critical for predicting safe service life. The focus of Savannah River National Laboratory's (SRNL) program on tritium impacts on structural materials is to gather data on the properties of stockpile relevant materials as tritium-decay-helium builds in order to inform lifetime assessment and prediction of tritium storage vessels. Further studies continue to improve the understanding of material performance over component lifetimes while new studies are required as novel materials and processes arise.

Tritium embrittlement has been studied at SRNL through tensile and fracture testing of austenitic stainless steel base metal forgings, providing necessary inputs for design guidance [6, 7]. These data, combined with testing at SNL/CA on hydrogen-precharged materials, have provided the basis of our current understanding of hydrogen-isotope embrittlement. SRNL's ongoing efforts with SNL/CA aim to address remaining gaps in our understanding of tritium embrittlement and thus support SNL in providing the experimental data necessary to develop quantitative models for describing tritium embrittlement and predicting component lifetimes. One such gap is in data on the fusion zones (FZ) and heat affected zones (HAZ) of welds. Another is the influence of the material's microstructure on tritium embrittlement. These studies will clarify underlying mechanisms of tritium embrittlement over a variety of helium concentrations through collaborative testing with SNL/CA.

Several studies are discussed in this report focusing on tritium/helium embrittlement; introducing new investigations or updating ongoing experiments.

1. Stainless 304L Tube Tensile Testing
2. Notched and Smooth tensile testing of 304L
3. Weld Fracture testing
4. New sample charging

Finally, progress on the application of the TPD technique is briefly noted.

2.0 Experimental Procedures

2.1 Type 304L Stainless Steel Tube tensile testing

Testing was conducted on commercially available 3.175 mm outer diameter 304L stainless steel tubing with 0.7 mm wall thickness. The nominal composition of the tubing as given by the manufacturer is shown in Table 2-1.

Table 2-1 – nominal 304L tube alloy composition (wt.%) from manufacturer

alloy	Cr	Ni	Mn	Mo	Si	C	S	P	Fe
304L	18.6	11.7	1.7	0.08	0.43	0.021	0.0004	0.017	Bal.

The type 304L tubing was received in a strain-hardened condition. Samples were heat treated to vary the microstructure and strength of the tubing without changing the composition. The heat treatment conditions were chosen to achieve five qualitatively different microstructural conditions: (i) partially recovered (866K / 60 min), (ii) fully recovered (1000 K / 30 min), (iii) partially recrystallized (1033 K / 30 min), (iv) fully recrystallized (1116K / 60 min), and (v) fully annealed (1311 K / 60 min). The microstructures of the as-received and heat treated materials are shown in Figure 2-1. The variety of tested microstructures is yielding information on the variation of tritium embrittlement with differing thermal histories.

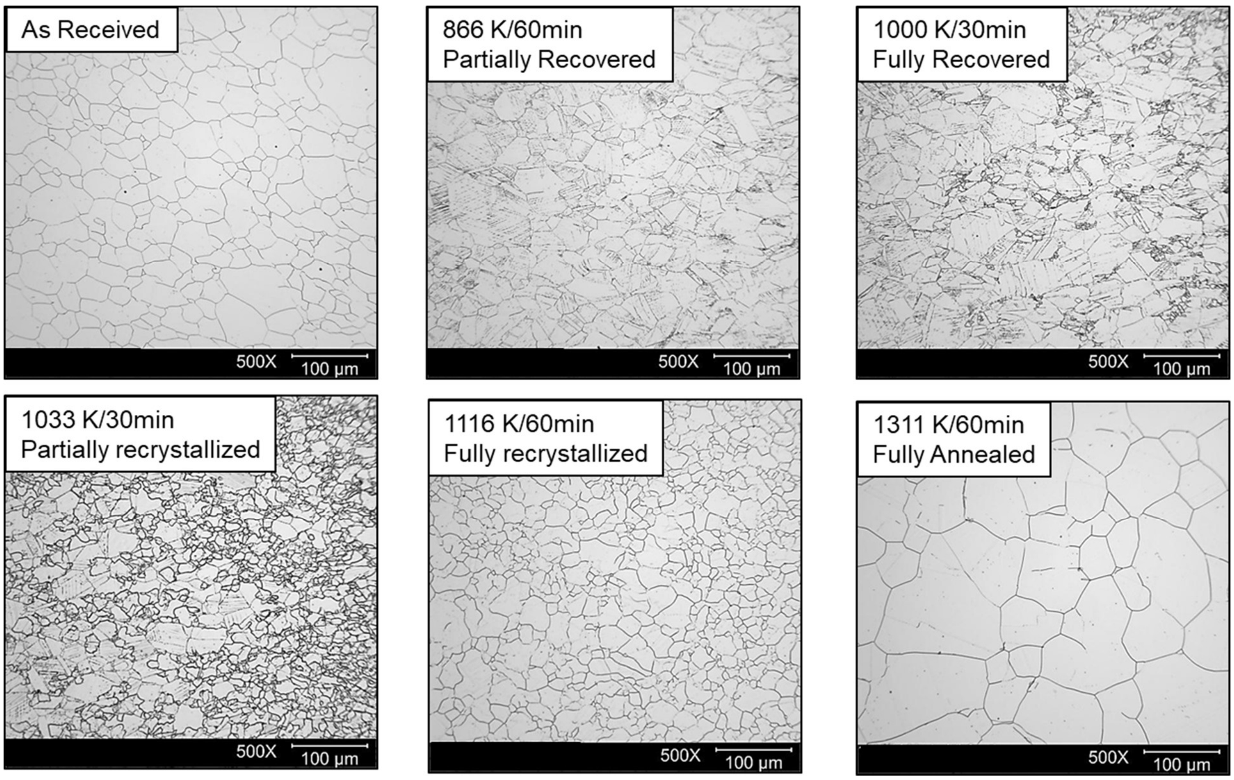

Figure 2-1 – micrographs of 304L tube microstructures based on different heat treatments. Further description in the text. Reproduced with permission from SNL/CA through SAND2020-8528 PE [8].

At SNL/CA, samples were thermally precharged with hydrogen at 138 MPa and 573 K for 10 days to allow uniform saturation of the tubes. Tritium precharging was conducted at SRNL at 34.5 MPa and 623 K for 14 days. At 573 K, uniform saturation of a solid cylinder with diameter of 3.175 mm would occur in 2-3 days; however, often times precharging runs contain multiple specimen geometries and the length of the precharging run is dictated by the largest sample. Therefore, the samples in both hydrogen and tritium were fully and uniformly saturated given the long precharging times. The tubes precharged with tritium were subsequently aged at low temperature (193 K) for 6 months to permit approximately 100 appm helium to accumulate in the material (along with a concomitant reduction in tritium content). We call this condition the tritium-aged condition to distinguish it from the hydrogen precharged condition. These two sets of charging conditions result in nominally 7700 and 3700 appm hydrogen and tritium respectively, due to the differences in pressures and temperatures. Additional details of the preparation and testing of samples in the non-charged and hydrogen-precharged condition are described in [9, 10].

The conditions of the tensile testing of the tritium-aged samples were nominally the same as for the non-charged and hydrogen precharged conditions. Tritium-aged specimens were tested at ambient laboratory conditions with a 25.4 mm gauge length extensometer and 2.54 mm/minute displacement rate in an electromechanical screw driven load frame, with each specimen tested to failure. Specimens were gripped over lengths of approximately 25.4 mm using pin inserts in the grip region to prevent tube collapse as suggested in ASTM E8. The test setup can be seen in the left panel of Figure 2-2.

2.2 Type 304L Stainless Steel Tensile Specimens

Samples of the type 304L stainless steel in the smooth tensile and notched tensile specimen geometries were supplied by SNL/CA.

Forged 304L tensile specimens (both smooth and notched) were tritium-precharged and aged to 100 appm helium followed by testing at SRNL. Notched tensile specimens experience complex triaxial stress state in testing enabling the study of the process of void nucleation, while smooth tensile specimens inform the development of flow curves of tritium embrittled material for computational modeling. Interrupted tests were also completed to enable microstructural characterization to advance understanding of deformation processes in tritium-exposed structural materials. The smooth and notched 304L tensile specimens were charged with tritium at 34.5 MPa and 350°C for two weeks in July 2019, achieving a nominal initial tritium content of 3700 appm in the 304L material. For more details on the conditions of the tritium pre-charging, refer to SRNL-STI-2018-00036 [6]. After charging, specimens were stored in a freezer at 0°C for 3 months and thereafter at -80°C, or in a radiological hood pending testing. Mechanical testing occurred in January and February of 2020, at which time, nominally 100 appm of helium had developed, leaving 3600 appm tritium. Typical test setups are shown in Figure 2-2.

Figure 2-2. SRNL's radiological hood with tube specimen (left) and tensile test setup (right) used in testing samples pre-charged with tritium

Tensile tests on the specimens described above were conducted at room temperature in air using a screw-driven testing machine in displacement control while measuring load, crosshead displacement, and extension. Smooth tensile specimens were tested with a 12.7 mm gauge length, 1.27 mm/minute displacement rate, and to 5%, 10%, and 20% true strain as well as to failure. Notched tensile specimens were tested with a 12.7 mm gauge length, 0.0254 mm/minute displacement rate, to a drop from peak load of 9% and 12%, as well as to failure.

2.3 Fracture testing of Welds and Heat Affected Zones

Previous reports (Annual aging studies report SRNL-STI-2018-00036, and SRNL-STI-2020-00002) discussed the preparation and initial fracture testing results from tritium-precharged 304L/308L FZ and HAZ and 21-6-9/308L FZ and HAZ samples aged to approximately 330 appm (304L HAZ and FZ and 21-6-9/308L FZ material) and 540 (21-6-9 HAZ material, due to higher tritium solubility) helium. Measured fracture properties decreased following the tritium charge and age, but to a lesser degree than in the hydrogen-precharged condition tested at SNL/CA. This is likely due to differences in total hydrogen-isotope concentration (e.g. SNL/CA precharges samples at higher pressures, resulting in higher hydrogen-isotope concentrations).

Longer aging conditions were tested in 2020 in the same fashion as reported in those previous reports, at approximately 3 years of aging, leading to nominally 600 and 980 appm helium in the 304L and 21-6-9 samples respectively. To investigate whether testing rate has an influence on measured fracture resistance, two different testing rates were examined: 0.002 mm/min and 0.02 mm/min. Previous work at SNL observed minimal differences in fracture resistance between these two testing rates with hydrogen [11]

2.4 New Sample Charging

Samples prepared by SNL/CA were tritium pre-charged at the Savannah River Tritium Facility from September 10th – October 2nd of 2020. Included in this charging were three specimen geometries: 1) 304L smooth tensile e-beam weld specimens, 2) 304L e-beam welded arc shaped fracture mechanics specimens, and 3) annealed 21-6-9 smooth tensile specimens. A list of the charged specimens follows in Table 2-2.

Table 2-2. Samples tritium pre-charged in … 2020

SNL Samples	**Material**	**Specimen ID**
Type 304L e-beam welds – smooth tensile	304L	4EW - [2-24] evens
Type 304L e-beam welds – arc fracture mechanics	304L	4EW – [1,3,5,7,13,19,21,23,25,27,29,31]
Type 21-6-9 annealed – smooth tensile	21-6-9	94L - [101-136]

After charging, specimens were transferred to SRNL facilities for storage at -80°C. These charging conditions are predicted to yield initial concentrations of 3700 atomic parts per million tritium (appm) in 304L specimens and 6100 appm tritium in 21-6-9 specimens, based on solubility calculations using data published by San Marchi et al [12]. Due to storage conditions, the samples were stored in a air hood at 20°C for 45 days, where after they were moved to a freezer for storage at -80°C.

Table 2-3, Table 2-4, and Table 2-5 describe the notional plan for aging and testing these samples. They are grouped as 304L smooth tensile e-beam weld specimens, 304L e-beam welded arc shaped fracture mechanics specimens, and annealed 21-6-9 smooth tensile specimens respectively and the storage times (aging) to reached desired He-3 levels are shown. Note that an additional "early" aging condition of 200 appm helium is being targeted for the annealed 21-6-9 samples as shown in Table 2-5. Previous testing has shown that fracture resistance of 21-6-9 decreases quite rapidly as a function of helium concentration. Targeting several lower helium concentrations is being pursued to better understand the degradation process.

Table 2-3. 304L smooth tensile e-beam weld specimens test matrix

Test	# of Specimens			
	100 appm He (~6mo)	**300 appm He (1.5 yr)**	**600 appm He (3 yr)**	**1000 appm He (5.6 yr)**
To failure	2	2	2	2
Interrupted	1	1	1	1

Table 2-4. 304L e-beam welded arc shaped fracture mechanics specimens test matrix

Test	# of Specimens			
	100 appm He (~6mo)	**300 appm He (1.5 yr)**	**600 appm He (3 yr)**	**1000 appm He (5.6 yr)**
Fracture center weld	3	3	3	3

Table 2-5. annealed 21-6-9 smooth tensile specimens test matrix

	# of Specimens				
	100 appm He (~3 mo)	200 appm He (~7 mo)	300 appm He (~1 yr)	600 appm He (~2 yr)	1000 appm He (3.18 yr)
Failure	3	3	3	3	3
5% (true strain)	2	2	2	2	2
20% (true strain)	2	2	2	2	2

3.0 Results and Discussion

3.1 304L tube tensile samples

The results in these section were presented at the 3rd Asia Pacific Symposium on Tritium Science, and have been submitted in a manuscript, "Tritium embrittlement of austenitic stainless-steel tubing at low helium contents" under review for publication [13].

Prior studies at Sandia National Laboratories on the effects of hydrogen [9, 10] demonstrated that internal hydrogen-induced losses in ductility could be correlated with differences in yield strength despite significant microstructural differences in compositionally identical material. Herein, the effect of tritium precharging and aging on the tensile response of type 304L tubing is presented. The materials were saturated with tritium at elevated temperature and subsequently aged at low temperature for 6 months, resulting in nominally 100 atomic parts per million (appm) of helium derived from tritium decay. Tritium precharging and aging for a short duration resulted in increased yield strengths, ultimate tensile strengths and slightly increased elongation to failure, comparable to higher concentrations of hydrogen precharging. Full results, engineering stress-strain curves, and discussion are in the publication process: as [13].

3.1.1 Results

The heat treatments resulted in microstructures as shown in Figure 2-1. Proceeding through the microstructural images in Figure 2-1, the "As Received" material has small, equiaxed grains. The "Partially Recovered" microstructure displays evidence of polygonization, but as is seen in the mechanical properties, the material only slightly softened. The "Fully Recovered" microstructure advances the recovery process further, while the "Partially Recrystallized" microstructure displays the beginning of the formation of new grains, with nominally complete recrystallization in the "Fully Recrystallized" microstructure. Finally, the "Fully Annealed" microstructure displays significant grain growth after recrystallization.

The tensile response of the non-charged samples are shown in Figure 3-1, as reported in [9, 10, 13]. Yield, ultimate tensile strength, and elongation values for all samples, as well as reduction of area measurements on non-charged and hydrogen-precharged samples, are tabulated in Appendix A. In every heat treatment condition, hydrogen precharging increases yield strength, averaging a 19% increase over the noncharged controls. The ultimate tensile strength also increases with hydrogen precharging, on average by 10%. Finally, elongation to failure also increases on average by 14%. While elongation may increase after hydrogen precharging, the reduction of area is always reduced by internal hydrogen. The tritium-aged condition shows comparable behavior to the hydrogen-precharged condition in each microstructure. Modest increases to yield (16%), ultimate tensile strength (5%), and elongation to failure (19%) were measured over the noncharged controls.

The yield and tensile strength of the tritium-aged condition is generally slightly lower than the hydrogen precharged condition. In considering these mechanical test results, it is important to note that the hydrogen precharging condition leads to a nominal hydrogen content of 7700 appm, while the tritium- aged condition retains 3600 appm of tritium and develops 100 appm helium. Recently published data demonstrate an approximately linear relationship between strength (as well as ductility) and hydrogen concentration [14]. As well, low levels of just a few hundred appm helium or less can have significant impacts on the fracture resistance of austenitic stainless steels [15]. Moreover, such low helium levels can lead to embrittlement similar to that seen in steels with significantly higher hydrogen isotope contents [16]. The measurements presented here qualitatively agree with these previous data, where the lower hydrogen isotope concentration in the tritium-aged condition is mostly offset by the hardening due to helium buildup.

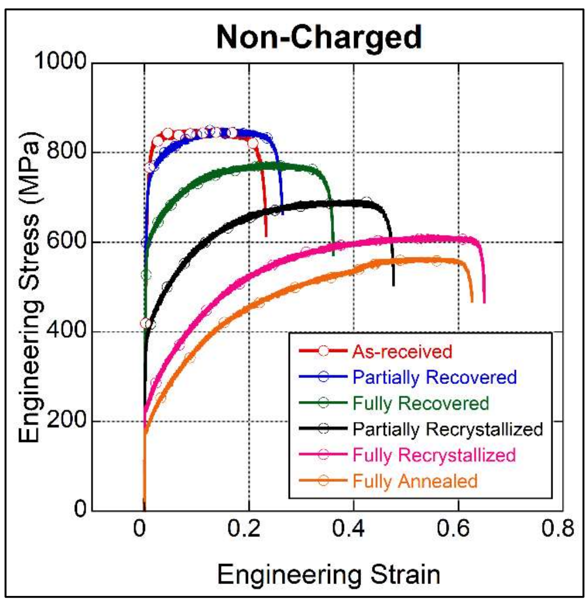

Figure 3-1 – Stress-Strain results from non-charged tube specimens. Reproduced from [13]

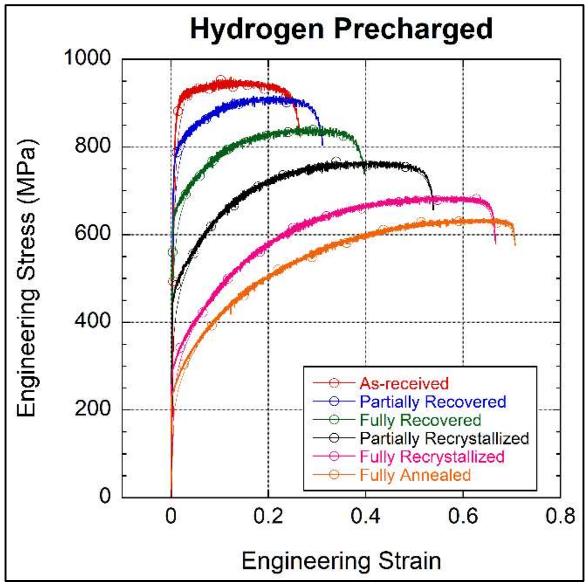

Figure 3-2 – Stress-Strain results from hydrogen precharged tube specimens. Reproduced from [13]

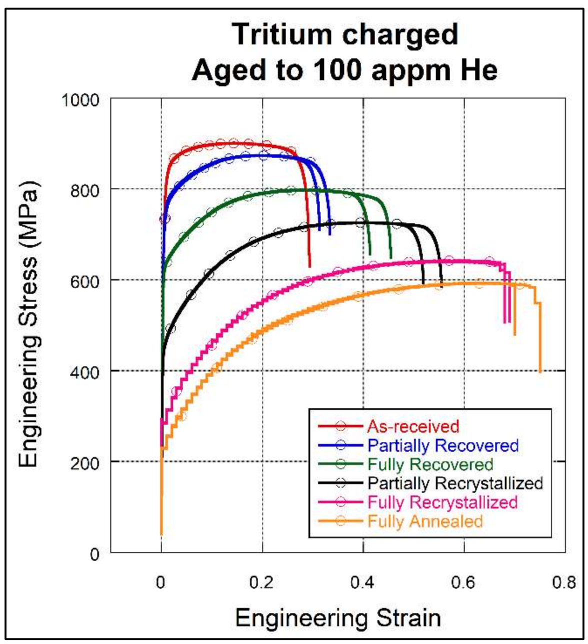

Figure 3-3 – Stress-Strain results from the first aging of tritium pre-charged tube specimens (6 months aging to attain ~ 100 appm helium). Reproduced from [13]

Finally, Figure 3-4 shows the percent change in yield strength over the noncharged condition for both hydrogen-precharged and tritium-aged samples. These data indicate some degree of microstructural dependence on the relative hardening due to hydrogen, where partially recovered microstructures are somewhat less sensitive to hydrogen, while more complete recrystallization and annealing is as sensitive or more sensitive than the strain hardened microstructure. The same systematic variation with microstructure is not seen for elongation or ultimate tensile strength. These results are preliminary, and more work is required to explain this behavior.

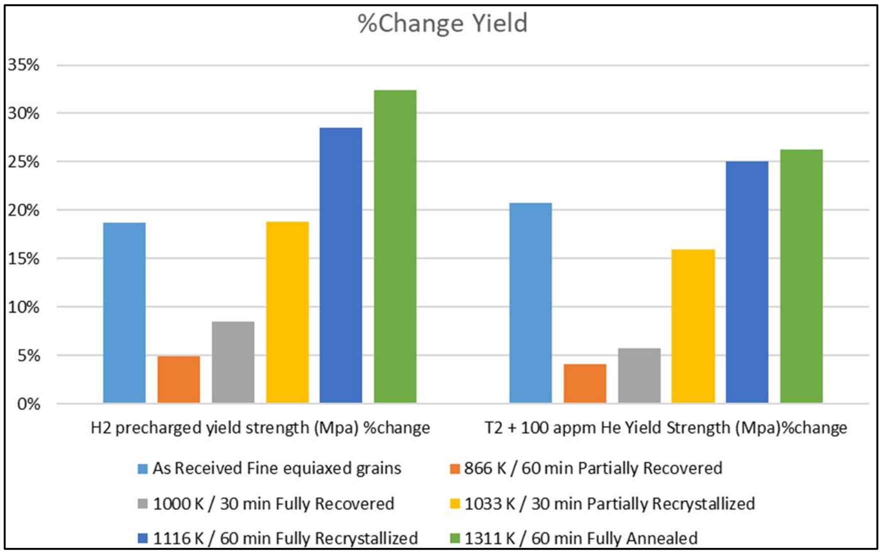

Figure 3-4 – Percent changes in yield strength over the noncharged condition for thermally hydrogen precharged and tritium precharged tube samples. Reproduced from [13]

3.1.2 304L Weld Tube Tensile Test Results

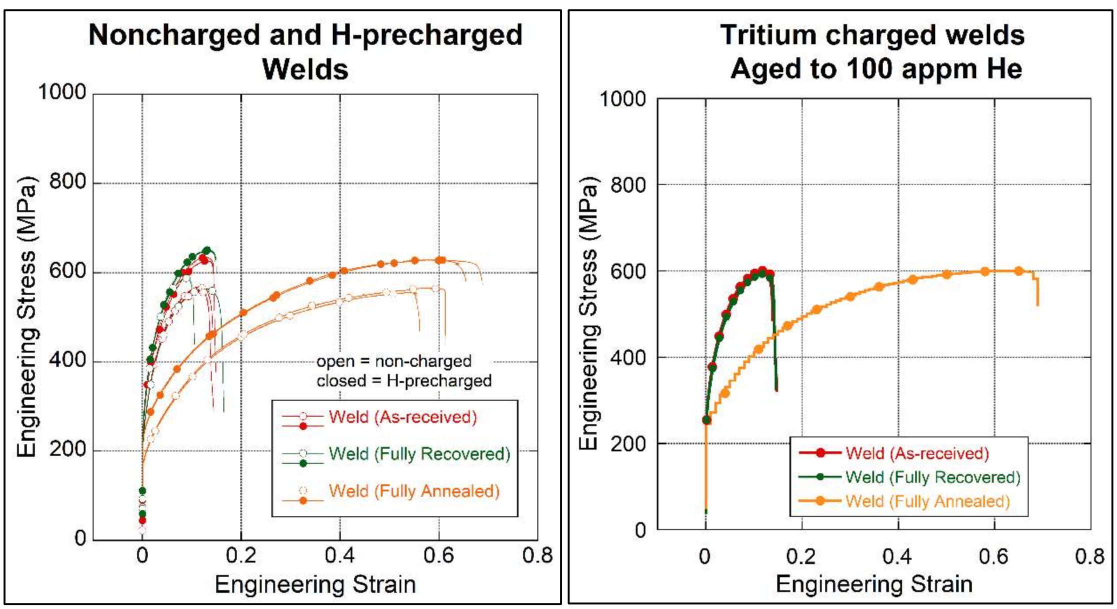

(a) (b)

Figure 3-5 - Stress-Strain results from (a) noncharged and H-precharged welds, and (b) the first aging of tritium pre-charged tube welds (6 months aging to attain ~ 100 appm helium). Reproduced from [13]

The welded samples exhibit interesting trends that highlight the mechanics of the specimens. The fusion zone of the weld has significantly lower strength than the base materials as shown in Figure 3-5 and as a consequence, the yield strength is dominated by the strength of the fusion zone, which is similar to the recrystallized material. The large difference between the strength of the base material and the fusion zone causes the deformation to be restricted to the fusion zone, because the stresses never exceed the yield strength of the base material. In the case of the welded, annealed tubing, the weld and base material have similar properties, thus the strength and ductility properties for all conditions reflect the behavior of the annealed tubing. Taken together, these observations suggest that the behavior of the welds in the helium-aged condition is analogous to the behavior of the annealed material in the same helium-aged condition.

3.2 304L notched and smooth tensile samples

3.2.1 Tensile Testing Results

Results from the smooth and notched tensile tests are shown in Figure 3-6. Note that the scales for smooth tensile specimens are normalized for geometry to give the material properties of Engineering Stress and Engineering Strain, while the data from notched tensile testing is shown with Load and Extensometer readings because the complex geometry doesn't allow for the same normalization. Tests on the smooth tensile coupons were either to nominally failure or interrupted at 5, 10, 20% strain. The tests to failure are being used to help develop and calibrate plastic flow models at SNL/CA for various amounts of helium content. A microscopy study will be performed on the interrupted smooth tensile coupons in order to understand how damage evolves with 100 appm helium in the microstructure. The notched tensile coupons were tested to either failure or interrupted immediately before failure. The notch provides elevated triaxial stress and will therefore affect the damage evolution compared to a smooth specimen. The notch is also a closer approximation to the behavior that would be expected near a crack. Therefore, microscopy investigations are planned on both the failed and interrupted notched samples to understand how damage evolves in this modified stress state. Further testing of these sample groups is scheduled for January 2021 to investigate helium levels of 300 appm, with higher concentrations of helium in subsequent experiments.

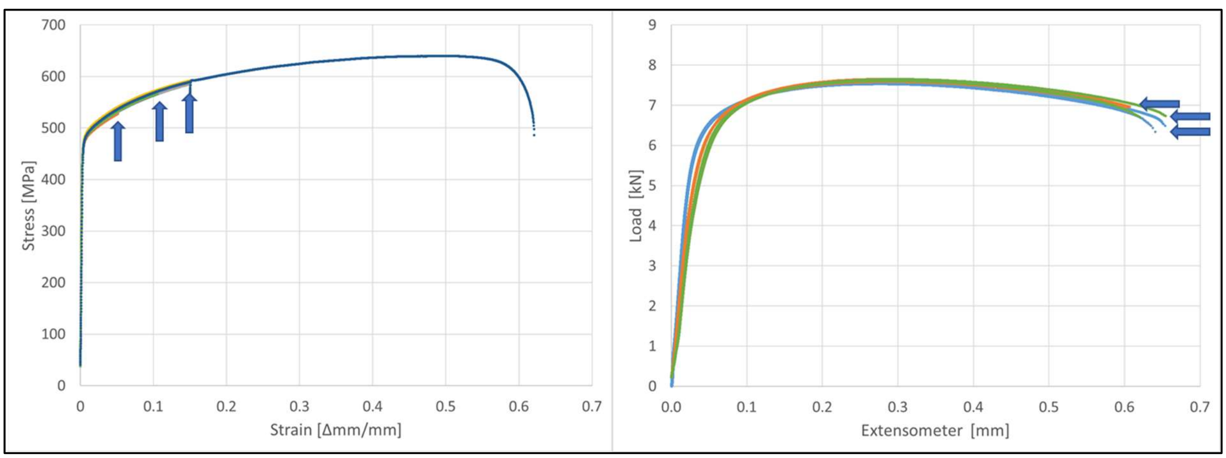

Figure 3-6 – Results from smooth tensile (left plot) and notched tensile (right plot) 304L stainless steel specimens pre-charged with 3700 appm tritium and aged to build in 100 appm helium. Blue Arrows on each are guides to point out the end of interrupted tests.

3.3 Fracture testing of Welds and Heat Effected Zones

Fracture testing at higher levels (nominally 600 and 980 appm helium in the 304L and 21-6-9 samples respectively) was conducted November of 2020 to further develop our understanding of helium concentration on fracture resistance in weldments and their heat affected zones. This testing was conducted in the same manner as the previous round of testing documented in SRNL-STI-2020-00002 which contained nominally 330 and 540 appm helium in the 304L and 21-6-9 samples, respectively. The effect of strain rate was examined in this round of testing. The first value reported for each sample was conducted at

0.002 mm/min while the other tests were conducted at 0.02 mm/min. Negligible differences were observed between the two testing rates. Rising displacement fracture resistance plots and low magnification fractography are presented at the end of the report in Appendix B.

Table 3-1 – Fracture Resistance values (J_Q [kJ/m^2]) for Weld and HAZ samples

Material	Nominal helium content (appm)	J_Q (kJ/m^2)	Average J_Q (kJ/m^2)
304L/308L Heat Affected Zone	600	311, 332, 337	327
21-6-9/308L Heat Affected Zone	980	101, 84	93
304L/308L Fusion Zone	600	168, 175, 88	144
21-6-9/308L Fusion Zone	600	183, 208, 171	187

Note - the leftmost J_Q *value is at 0.002 mm/min, all others at 0.02 mm/min rate*

Table 3-2 – Fracture Resistance as a Function of Helium content

Material	Nominal helium content (appm)	Fracture Resistance (kJ/m^2)
304L/308L Heat Affected Zone	330	424
	600	327
21-6-9/308L Heat Affected Zone	540	132
	980	93
304L/308L Fusion Zone	330	155
	600	144
21-6-9/308L Fusion Zone	330	226
	600	171

3.4 Thermally Programmed Desorption

Installation and commissioning of a new ultra-high vacuum (UHV) system outfitted with a high resolution Extrel mass spectrometer was completed (Figure 3-7). This instrument will support the Aging and Lifetimes program by providing mass resolution previously not available, allowing accurate determination and identification of hydrogen isotopes under UHV conditions. Following successful commissioning of the instrument, initial sample testing is now underway. Preliminary measurements are focused on hydrogen charged and uncharged legacy stainless steel samples. Initial results, shown in Figure 3-8, display a clear increase in hydrogen concentration for the charged stainless steel sample. Routine testing is set to begin in early January 2021, with a planned expansion of the instruments capabilities to include powder hydride samples using a custom designed sample holder.

Figure 3-7. Extrel TPD System

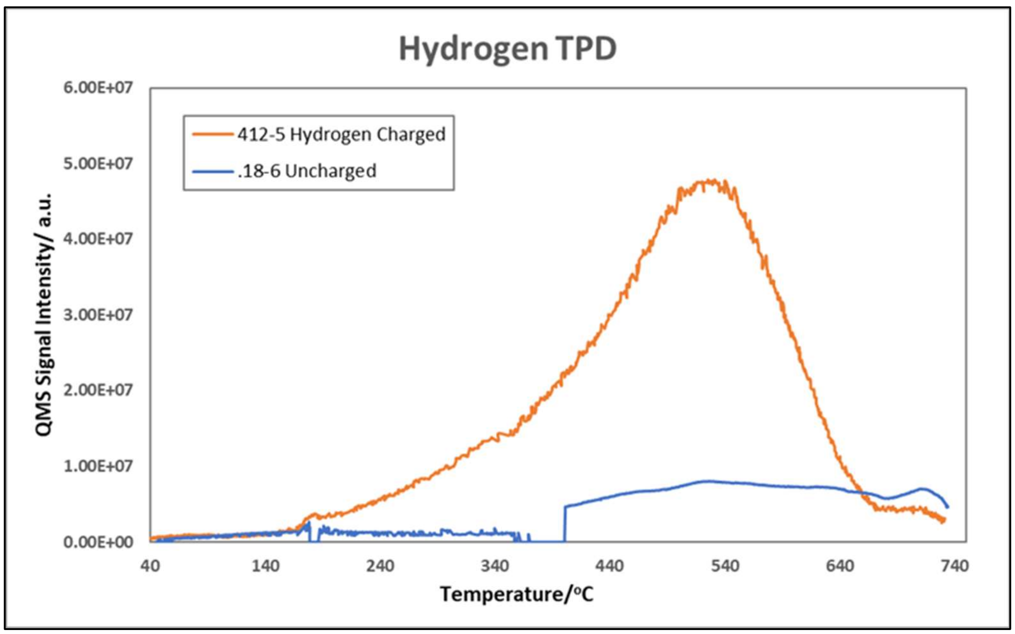

Figure 3-8. Hydrogen TPD comparing hydrogen charged (orange line) and uncharged (blue line) 304L stainless steel samples.

4.0 Summary and Conclusions

- Tensile testing on 304L in tubes, notched tensiles, and smooth tensiles were completed following tritium precharging and aging to nominally 100 appm helium. Tritium precharged samples exhibited similar tensile behavior to hydrogen precharged samples with comparable hydrogen-isotope concentrations. Low levels of helium (i.e. 100 appm) did not appear to significantly degrade the tensile ductility. Additionally, evidence of some dependence of embrittlement on the specific microstructural condition was identified and warrants additional research. Tensile samples will be aged longer and tested in out years to evaluate the effects as higher helium content is built in.

- Fracture tests from 304/308L and 21-6-9/308L welds and HAZ were conducted at a longer aging condition to complement shorter aging conditions reported previously. Fracture resistance decreased at longer aging conditions, where more helium has developed in the material. The 21-6-9/308L HAZ exhibited the greatest degradation in fracture resistance. Targeted studies were initiated this year to examine 21-6-9 steel to try and elucidate the mechanism of the more pronounced degradation due to helium.
- Tritium precharging was conducted this year on annealed 21-6-9 tensile specimens and 304L electron beam welded tensile and fracture specimens. Mechanical testing of these samples at low helium concentrations is scheduled in 2021.

5.0 References

[1] G. R. Caskey, "Hydrogen Effects in Stainless Steel," in *Hydrogen Degradation of Ferrous Alloys*, R. A. Oriani, J. P. Hirth, and M. A. Smialowski, Eds., ed Park Ridge, NJ: Noyes Publishing, 1985, pp. 822-862.

[2] G. Caskey Jr, "Tritium-helium effects in metals," *Fusion Technology,* vol. 8, pp. 2293-2298, 1985.

[3] S. L. Robinson and G. J. Thomas, "Accelerated Fracture due to Tritium and Helium in 21-6-9 Stainless Steel," *Metallurgical Transactions A,* vol. 22A, pp. 879-885, 1991.

[4] S. L. Robinson, "The Effects of Tritium on the Flow and Fracture Stress of Austenitic Stainless Steels," in *Hydrogen Effects on Material Behavior*, N. R. Moody and A. W. Thompson, Eds., ed Warrendale PA: TMS, 1990, pp. 433-445.

[5] S. Robinson and N. Moody, "The effect of hydrogen, tritium and decay helium on the fracture toughness of a stainless steel superalloy," *Journal of Nuclear Materials,* vol. 140, pp. 245-251, 1986.

[6] M. J. Morgan, D. Hitchcock, T. Krentz, J. McNamara, and A. Duncan, "2017 Accomplishments–Tritium Aging Studies on Stainless Steel Weldments and Heat-Affected Zones," SRNL-STI-2018-00036 Savannah River Site (SRS), Aiken, SC (United States)2018.

[7] T. M. Krentz, D. A. Hitchcock, M. J. Morgan, J. A. Ronevich, R. Sills, C. San Marchi*, et al.*, "Fracture Toughness Properties of Tritium-Charged-and-Aged Stainless Steels: SRNL and SNL Collaboration Test Plan and 2018 Results," SRNL-STI-2019-00022 Savannah River National Laboratory, Aiken, SC (United States)2019.

[8] L. A. Hughes and e. al, "Title," unpublished|.

[9] L. A. Hughes, B. P. Somerday, D. K. Balch, and C. San Marchi, "Hydrogen Compatibility of Austenitic Stainless Steel Tubing and Orbital Tube Welds," in *International Conference on Hydrogen Safety (ICHS)*, Brussels, Belgium, 2013.

[10] L. A. Hughes, B. P. Somerday, D. K. Balch, and C. San Marchi, "Hydrogen compatibility of austenitic stainless steel tubing and orbital tube welds," *International Journal of Hydrogen Energy,* vol. 39, pp. 20585-20590, 2014.

[11] J. A. Ronevich, B. P. Somerday, C. W. San Marchi, and D. K. Balch, "Fracture threshold measurements of hydrogen precharged stainless steel weld fusion zones and heat affected zones," in *ASME 2015 Pressure Vessels and Piping Conference*, 2015.

[12] C. San Marchi, B. P. Somerday, and S. L. Robinson, "Permeability, Solubility, and Diffusivity of Hydrogen Isotopes in Stainless Steels at High Gas Pressures," *International Journal of Hydrogen Energy,* vol. 32, pp. 100-116, 2007.

[13] T. K. Krentz, J. A. Ronevich, D. K. Balch, and C. San Marchi, "Tritium embrittlement of austenitic stainless-steel tubing at low helium contents," *Manuscript Submitted for Publication,* 2020.

[14] C. San Marchi, J. A. Ronevich, J. E. C. Sabisch, J. D. Sugar, D. L. Medlin, and B. Somerday, "Effect of microstructural and environmental variables on ductility of austenitic stainless steels," *International Journal of Hydrogen Energy,* 2020.

[15] M. J. Morgan and M. H. Tosten, "Tritium Effects on Weldment Fracture Toughness," Savannah River National Laboratory, Washington Savannah River Company, Savannah River Site, Aiken, SC, USA No. WSRC-STI-2006-00056, 2006.

[16] M. Morgan, S. Scott West, and M. Michael Tosten, "Tritium and Decay Helium Effects on the Fracture Toughness Properties of Stainless Steel Weldments," in *8th International Conference on Tritium Science and Technology*, Rochester, New York 2007.

Appendix A. Tabulated test results from tensile testing

Table 5-1 – Mechanical Properties of 304L tubing (n/m = not measured). Includes hydrogen test data from SNL/CA for completeness, reproduced from [8-10]

Microstructure	Environmental condition (wt ppm)	Yield Strength (MPa)	Tensile Strength (MPa)	Total Elongation (%)	Reduction of Area
Strain-hardened (as-received)	Non-charged	697	857	23	0.71
	H-precharged	788	945	27	0.50
	T + He	802	907	27	n/m
Partially recovered	Non-charged	678	854	27	0.68
	H-precharged	711	915	32	0.50
	T + He	706	874	34	n/m
Fully recovered	Non-charged	576	780	36	0.64
	H-precharged	625	850	41	0.54
	T + He	609	798	45	n/m
Partially recrystallized	Non-charged	377	692	47	0.70
	H-precharged	448	770	53	0.58
	T + He	437	726	54	n/m
Fully recrystallized	Non-charged	228	614	63	0.76
	H-precharged	293	688	67	0.65
	T + He	285	641	69	n/m
Annealed	Non-charged	179	565	64	0.80
	H-precharged	237	636	71	0.66
	T + He	226	593	74	n/m

Table 5-2 – Mechanical Properties of 304L welded tubing. Includes hydrogen test data from SNL/CA for completeness, reproduced from [8-10]

Microstructure	Environmental condition (wt ppm)	Yield Strength (MPa)	Tensile Strength (MPa)	Total Elongation (%)	Reduction of Area
As-received tubing welded	Non-charged	248	566	15	0.82
	H-precharged	287	631	15	0.62
	T + He	287	600	15	n/m
fully recovered tubing welded	Non-charged	256	577	16	0.82
	H-precharged	296	651	15	0.67
	T + He	281	594	15	n/m
annealed tubing welded	Non-charged	178	561	59	0.78
	H-precharged	239	630	67	0.65
	T + He	239	601	68	n/m

Appendix B: Compiled weld bend bar fracture toughness testing results

HAZa – 304L/308L heat affected zone specimens

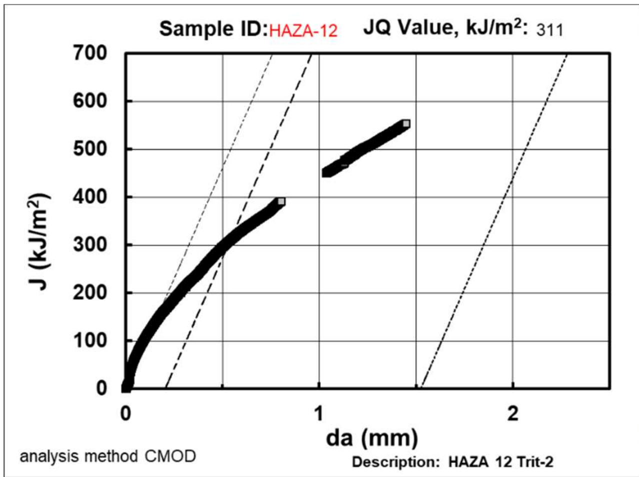

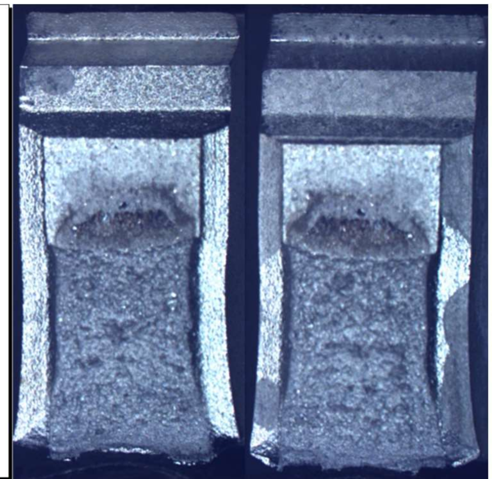

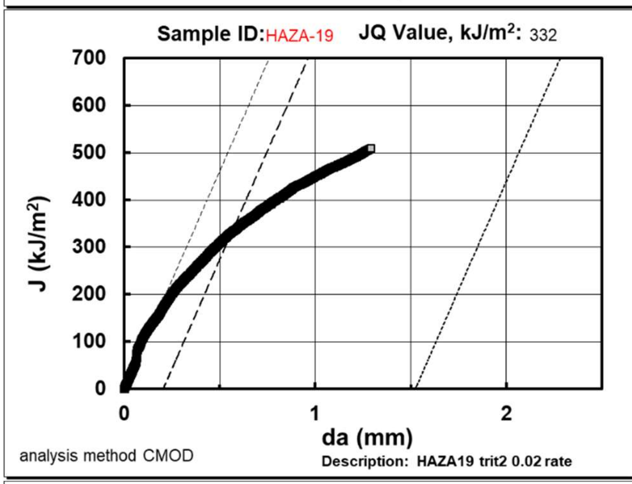

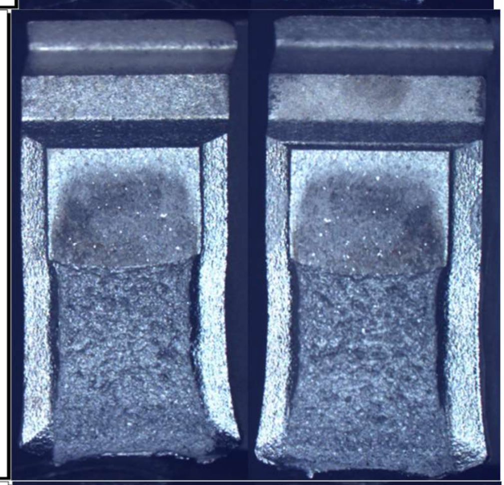

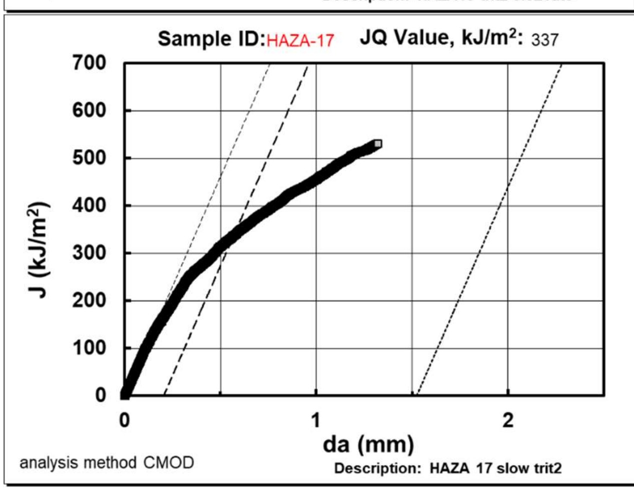

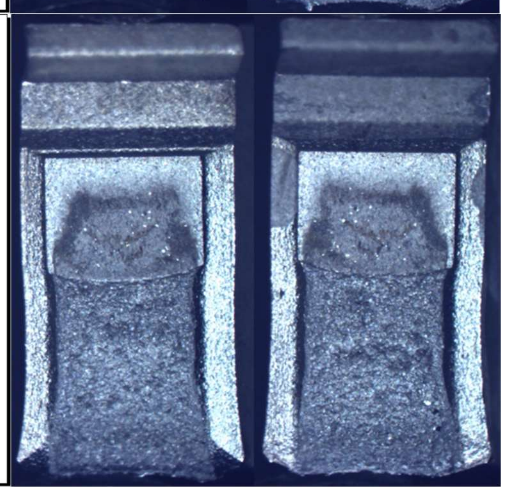

HAZb – 21-6-9/308L heat affected zone specimens

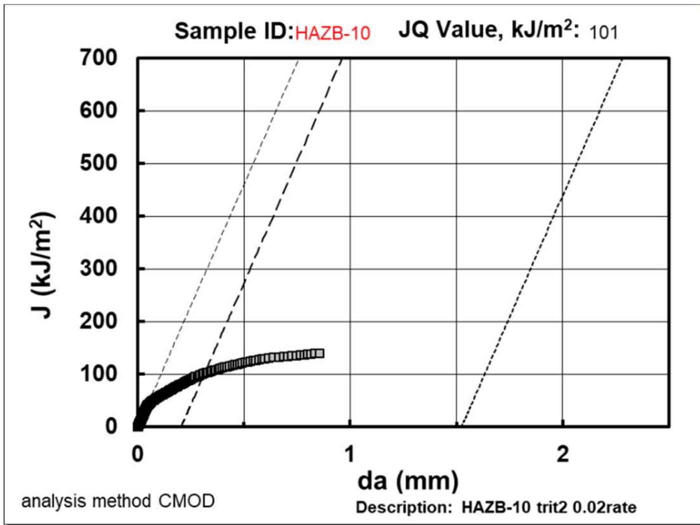

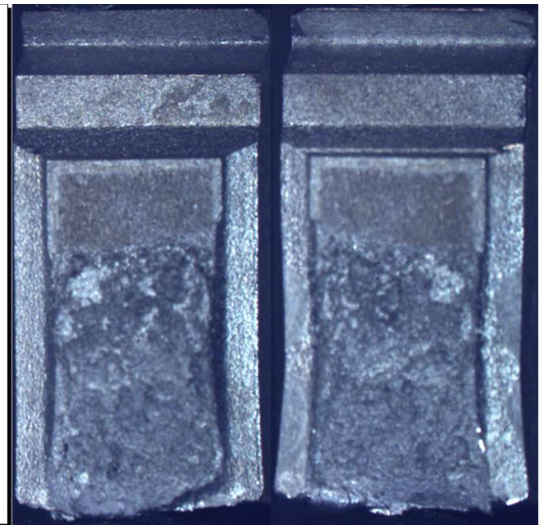

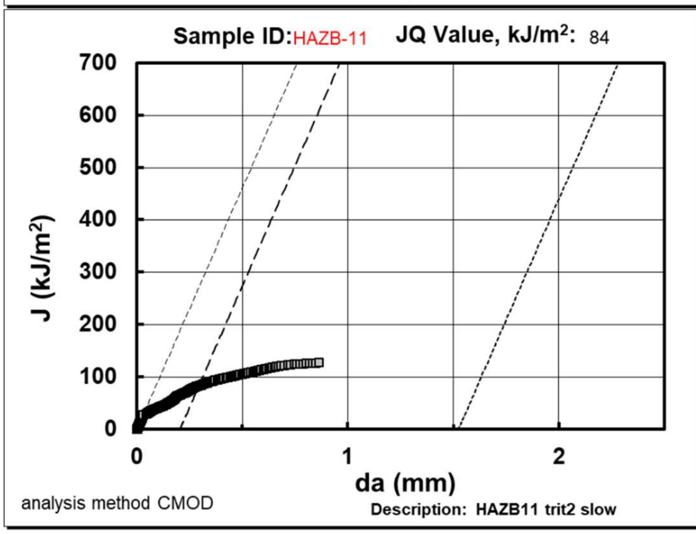

4FZ - 304L/308L fusion zone specimens

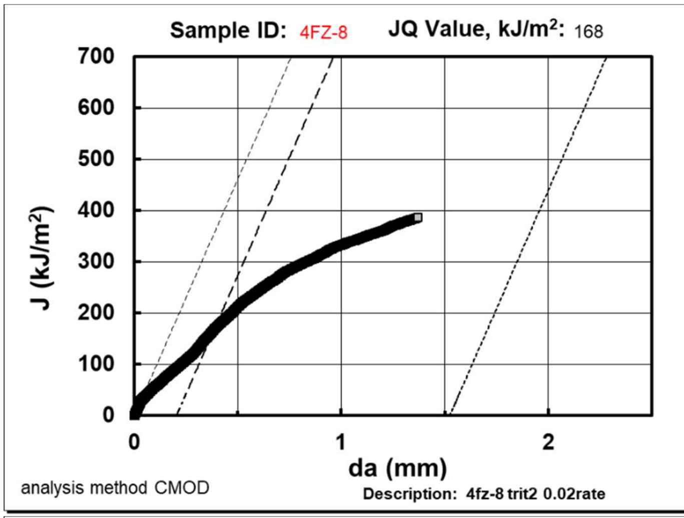

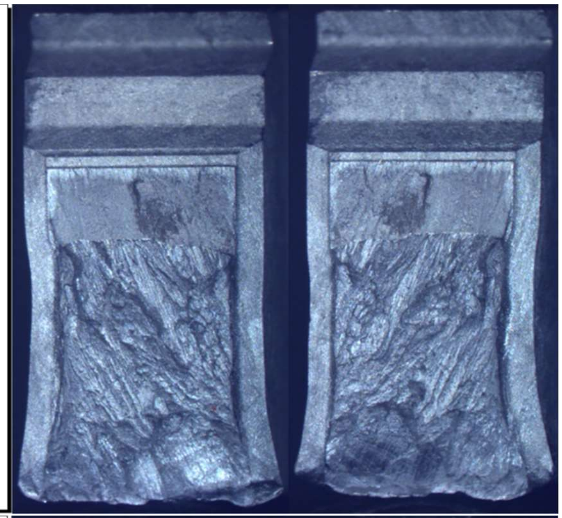

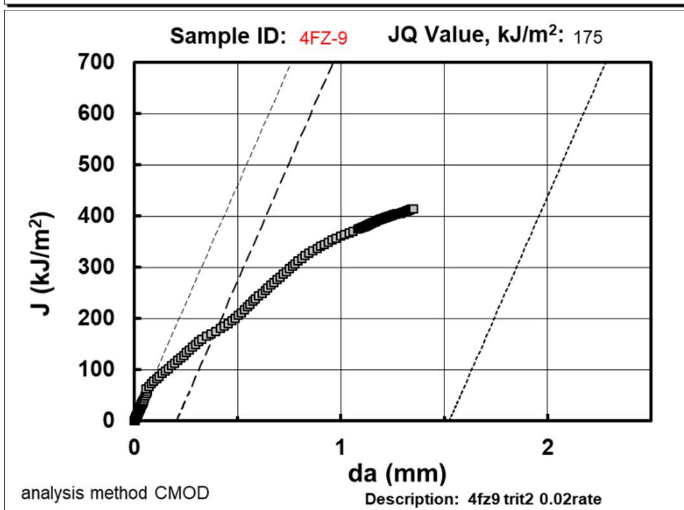

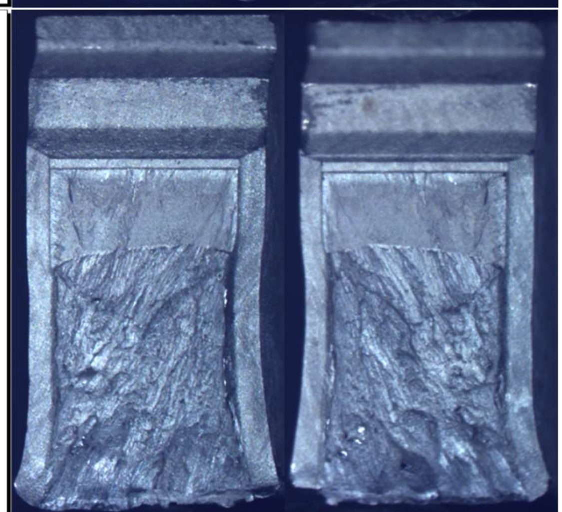

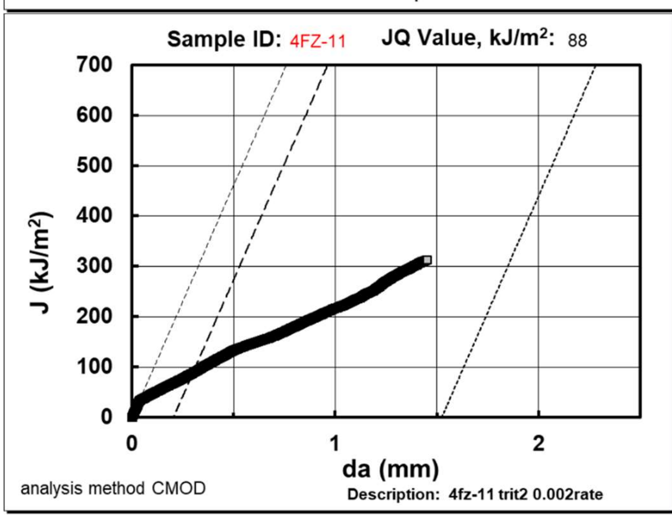

9FZ – 21-6-9/308L fusion zone specimens